UNITED NATIONS EDUCATIONAL, SCIENTIFIC AND CULTURAL ORGANIZATION
INTERNATIONAL CENTRE FOR THEORETICAL PHYSICS
I.C.T.P., P.O. BOX 586, 34100 TRIESTE, ITALY. CABLE CENTRATOM TRIESTE

H4.SMR/449-15

WINTER COLLEGE ON HIGH RESOLUTION SPECTROSCOPY

(8 January - 2 February 1990)

MULTIPHOTON IONISATION EXPERIMENTS WITH INTENSE SHORT PULSES

II

ATOMIC STRUCTURE IN INTENSE ELECTROMAGNETIC FIELDS

P. Agostini

Service de Physique des Atomes et ds Surfaces
CEN Saclay 91190
Gif Sur Yvette
France

MULTIPHOTON IONIZATION EXPERIMENTS WITH INTENSE SHORT PULSES

P. AGOSTINI

Service de Physique des Atomes et des Surfaces
CEN SACLAY 91190 GIF SUR YVETTE

II

Atomic Structure in Intense Electromagnetic Fields

I. Introduction
II. Stimulated Corrections to bound states
III. Multiphoton ionization in intense ultra short pulses
IV. Electron Spectroscopy with ultra short pulses
V. Intensity and Polarization dependence in MPI of xenon
VI. Linear Giant Stark Shifts

Atomic Structure in Intense Electromagnetic Fields

1. Introduction.

The interaction between charged particles and electromagnetic fields can be expanded according to powers of the coupling constant $e^2/\hbar c$. The terms of order larger than one are called "radiative corrections". They lead to well-known difficulties in QED since a straightforward evaluation results in infinite quantities. These difficulties have been solved by the procedure of renormalization of mass and charge of the electron, the self-mass and the self-charge being unobservable. However, if the electron is placed in an external field, the radiative corrections become observable: if the external field is a Coulomb field, the energy levels are displaced; if the external field is a constant magnetic field, the electron has an energy different from the one corresponding to its magnetic moment $e\hbar/2mc$. The correct prediction of these two effects (Lamb shift and anomalous magnetic moment of the electron) are among the most impressive successes of QED. These corrections are purely quantum mechanical in nature since they are due to vacuum fluctuations and polarization. They can be termed "spontaneous" radiative corrections. Closely related to them, are the "stimulated" radiative corrections of energy levels when the atomic system is placed in a strong external electromagnetic field. This displacement is also called AC-Stark shift, or dynamical Stark shift and is connected to the dynamical polarizabilities of the states. On the one hand, such corrections occur most naturally during multiphoton ionization transitions which are

observable only under strong field irradiation. On the other hand the study of multiphoton ionization offers an experimental method to investigate stimulated radiative corrections. However, energy levels are not only displaced by the electromagnetic field but also broadened. The broadenings of all levels, and, consequently, of all multiphoton lineshapes which would allow a measurement of the shifts, put a limit to such measurements. It is only very recently that it was discovered that electron spectroscopy, associated to subpicosecond pulses, could provide information on strongly displaced atomic energy levels. The first observations, which revealed the effect, were made with a fixed laser wavelength. They have been subsequently extended by the use of a tunable femtosecond laser source: this allows to measure the intensity dependence of the shifts in a range where all other methods fail. The results of these investigations are surprisingly simple. It appears that, under strong laser irradiation (10^{13}-10^{14} W cm^{-2}), the atomic spectrum is essentially stretched by several electronvolts: all the excited states being up-shifted by about the same amount. However, such a simplistic picture is probably not entirely true as recent non-perturbative calculations tend to show. It is likely that more experiments are needed to fully understand the behavior of atomic structure in intense electromagnetic fields. The aim of this lecture is to provide an overview of this recent aspect of multiphoton ionization. It is organized as follows: first, I review the theory of stimulated radiative corrections both in the

perturbative and non-perturbative regimes. Then I briefly recall the basics of multiphoton ionization with special emphasis on resonant transitions and Stark-induced resonances. I will show how Above-Threshold ionization can be used as a probe of the ionization threshold. I will then proceed to electron spectroscopy with ultrashort pulses, discuss the problem of assigning the various resonances which appear as structures in the photoelectron energy spectra and establish the necessity of using a tunable laser to get an essential information: the intensity dependence of the shifts. I will finally expose and discuss the recent experiments in Xenon.

I. Stimulated Corrections (ac-Stark Shifts) to Ground states.

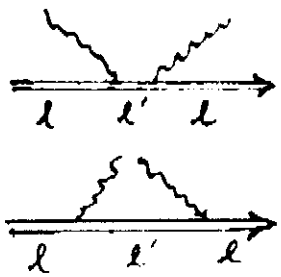

fig 1.

To second order in perturbation theory, the stimulated radiative correction is due to the two diagrams of fig 1. The energy change of state l due to coupling to states l' is given by:

$$\Delta E_l^{(2)} = \frac{-e^2 E^2 \hbar^2}{2m} \sum_{l' \neq l} \frac{f_{ll'}}{(E_l - E_{l'})^2 - (\hbar\omega)^2} \qquad (1)$$

where E, ω are the field strength and frequency and $E_l, E_{l'}$ the unperturbed energies of states l and l'; $f_{ll'}$, oscillator strength. Two limiting cases are of interest for multiphoton ionization. In the <u>quasi-static</u> limit ($\hbar\omega \ll E_l - E_{l'}$), the shift $\Delta E_l^{(2)}$

reduces to

$$\Delta E_\ell^{(2)} \simeq - \alpha_\ell I \qquad (2)$$

where α is the static polarizability of state ℓ. This approximation holds for the atom ground state if the photon energy is much smaller than the energy of the lowest excited state (ex: Xenon, $\lambda = 1.06\,\mu m$). As a consequence, the shift, in this case, is negative and small.

In the <u>high-frequency</u> limit ($\hbar\omega \gg E_\ell - E_{\ell'}$), expression (1) becomes by application of the sum-rule for $f_{\ell\ell'}$:

$$\Delta E_\ell^{(2)} \simeq \frac{e^2 E^2}{2 m \omega^2} \qquad (3)$$

The physical interpretation of (3) is very simple: the high frequency condition holds, for instance, for Rydberg states and optical frequencies. In this case, the electron is quasi-free and (3) represents the classical kinetic energy of the oscillatory motion of a free electron in an electromagnetic field E: it is positive and large.

In the <u>general case</u>, it is necessary to take into account the specific coupling of state ℓ to various states ℓ' in order to compute the shift. It may happen, however, that two particular states are strongly coupled if $E_\ell - E_{\ell'} \simeq \hbar\omega$ and $f_{\ell\ell'} \neq 0$. In this case the sign of the shift depends on ω through a <u>dispersion-like function</u>. If $\omega > \omega_{\ell\ell'}$ the two states are attracting each other while for $\omega < \omega_{\ell\ell'}$ they are repelling each other.

The Stark shifts have two important consequences regarding the ionization of atoms by multiphoton absorption. Firstly, once

to the combined effects of the ground state shift (negative and small) and Rydberg states shifts (positive and large), the ionization potential is increased by

$$\alpha_g I + \alpha_p I \qquad (4)$$

where $\alpha_p = 0.9410^{-13} \lambda^2$ (I in $W cm^{-2}$, λ in μm, shift in eV). ('p' stands for 'ponderomotive' as discussed below).
Secondly, the ionization probability may be enhanced, at particular intensities, by Stark-induced resonances. This will happen if the energy of a shifted state $\tilde{E}_R = E_R + \Delta E_R$ becomes equal to the energy of an integer number of photons.
The combination of Stark induced resonances and increase of the ionization potential result in observable effects on the energy spectra of photoelectron produced by multiphoton ionization with ultra short pulses and provide a method to measure the distortion of atomic structure in intense electromagnetic fields.

III. Multiphoton ionization in intense ultra short pulses

The question to be discussed in this section is the following: What are the consequences of the various radiative corrections just mentioned on the energy spectra of photoelectrons produced in multiphoton ionization?
To begin with, let us recall that, even at intensities at which radiative corrections are negligible, the photoelectron energy spectrum

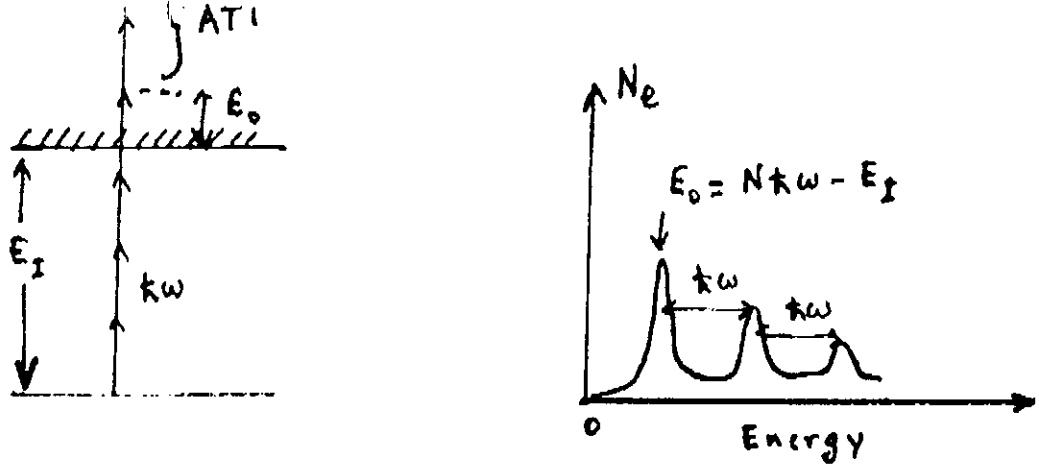

fig 2.

shows not only a peak at energy $E_0 = N\hbar\omega - E_I$, as expected from generalized Einstein's law (see notation in fig. 2), but displays a series of peaks separated by the photon energy $\hbar\omega$. This is the so-called "Above-Threshold Ionization" (ATI) process (See fig 2). Let us first examine the consequences of the increase of the ionization potential on such a spectrum. As the intensity is increased, the energy of the first peak becomes:

$$\tilde{E}_0 = N\hbar\omega - \tilde{E}_I = N\hbar\omega - E_I - (\alpha_g I + \alpha_p I) \quad (5)$$

The same change applies to all peaks which, therefore are all shifted towards low energies by the amount $(\alpha_g + \alpha_p) I$. Second, if the quantity $(\alpha_g + \alpha_p) I$ becomes comparable or larger than $\hbar\omega$ it follows that the corresponding peak is relatively suppressed. These two effects are easily observed if the experiment is carried out with "short" pulses. Let us suppose now that the light pulse is strong enough to shift a state of energy E_R into resonance:

$$\tilde{E}_R = p\hbar\omega = E_R + \Delta E_R \simeq E_R + \alpha_R I_R \quad (6)$$

The ionization probability is peaked around the intensity

$$I_R = \frac{p\hbar\omega - E_R}{\alpha_R} \qquad (7)$$

As a consequence most electrons are released around the energy (cf eq (5)):

$$E = N\hbar\omega - E_I - \frac{\alpha_q + \alpha_p}{\alpha_R}(p\hbar\omega - E_R) \qquad (8)$$

Eq (8) shows that the electron spectrum will have a maximum at one energy E, <u>independant</u> of the light pulse peak intensity. In fact, the intensity (7) is reached twice during the light pulse during the rise and fall of the pulse. The electrons with energy E are released at those instants. In reality, a careful analysis of the ionization reveals that these electrons come from regions of the ionization volume where the intensity (7) is reached at the maximum of the pulse. In any case, the electron energy spectrum maps the intensity dependence of the probability. Furthermore, the spectra are, to a large extent, independant of the pulse peak intensity.

It is important to remark that only "short" pulses allow to observe such electron energy spectra. • If, on the contrary, "long" pulses are used, the photoelectron kinetic energy is changed by the work of the Lorentz force along the electron trajectory through the field gradient. This force has a peculiar

component called the "ponderomotive force" whose work exactly compensates for the energy shift $\alpha_p I$.

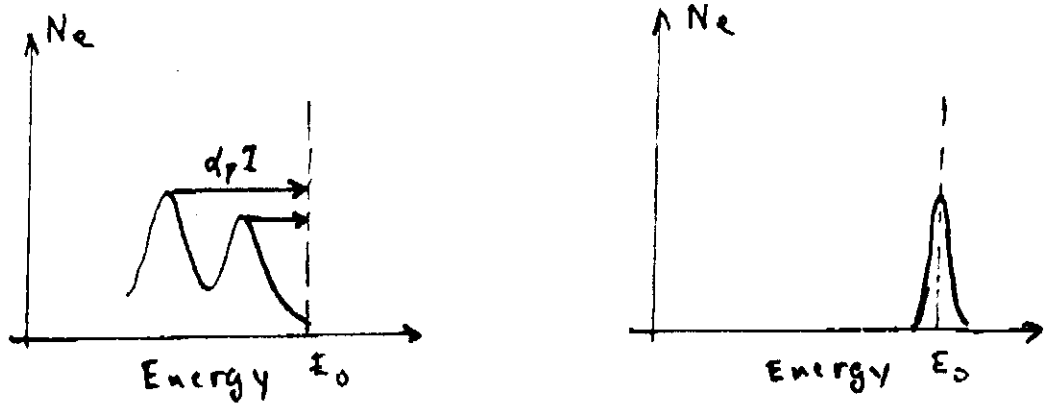

fig. 3

Figure 3 a) and b) shows how a spectrum showing resonances in the case of short pulses (a) contracts into a single peak in the case of long pulses (b). In this sense, a pulse is "long" if the electron has enough time to travel out of the field before the field distribution has significantly changed. In other words, the pulse duration τ must be much longer than the electron exit time $\frac{\phi}{v}$ where ϕ is the beam diameter and v the electron initial velocity.

IV Electron Spectroscopy with ultra-short pulses.

Among the various techniques which can be used to record photoelectron energy spectra, the time-of-flight method is particularly well adapted to short pulses. The electrons are produced during the laser pulse, at $t=0$, during a very short time. Then, they travel freely in a field-free space

to a detector located at a known distance L and the arrival time T is recorded by a digital oscilloscope or similar device. The main advantages of this method are the simplicity and the "multichannel" character: the detector records all the events between 0 and some maximum time determined either by the lowest energy compatible with stray fields or by the maximum memory capacity of the recording device. In other methods, to achieve such a spectral range, either several detectors or scanning of some field (electric or magnetic) would be required. The main drawback of the time-of-flight technique is the non-linear relationship between time and energy and, accordingly, a resolution which depends on energy. This is clearly seen from the fact that, usually, resolution is constant in time since it depends on the sampling bandwidth of the digitizer. As a consequence, in practice, the time-of-flight spectrometer is characterized by its time resolution and some maximum energy (for a given energy resolution). For instance if the sampling is done at 100 MHz ($\Delta T = 10$ ns) and if the flight distance is 50 cm, the maximum energy allowing a resolution of 0.1 eV is about 3 eV.

Another important characteristic of an electron spectrometer is its collection efficiency. This is specially important since,

to avoid space-charge problems, the total number of electrons produced for each laser pulse must be limited to about 100.

One elegant solution to obtain a high collection efficiency is the use of a strong magnetic field. Practically, a magnetic collection spectrometer is built as show in fig. 4

fig. 4

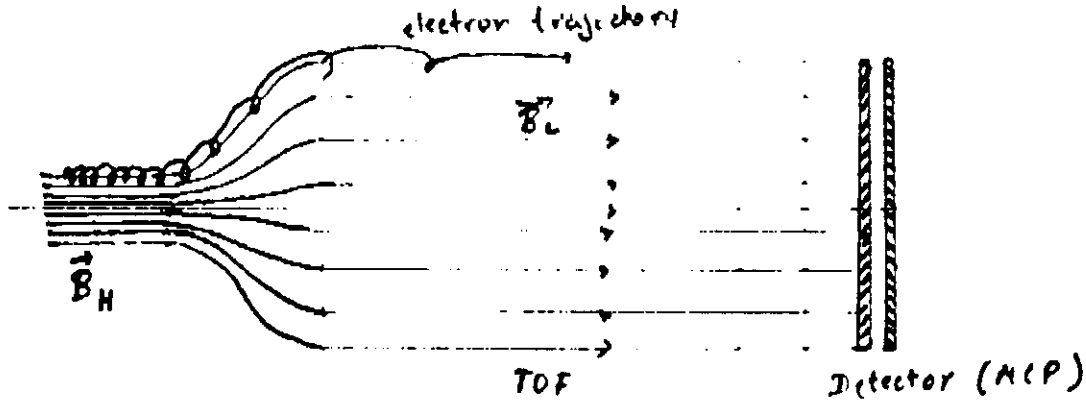

A region of high field (typically 1 Tesla) B_H, where the electrons are "created" is smoothly connected to a region of low field (10^{-3} T) B_L, both fields being parallel to the time-of-flight axis. Electrons with energies up to 10 eV are collected over a solid angle of 2π by the strong field and guided to the detector along the field lines of the low field (see fig 4).

Such a device has been used to analyse photoelectrons produced in multiphoton ionization of xenon by 120 femtosecond (10^{-13} s) pulses at 615 nm and to study the intensity and polarization dependence of the spectra. Figure 5 shows a schematic diagram of relevant energy levels in xenon.

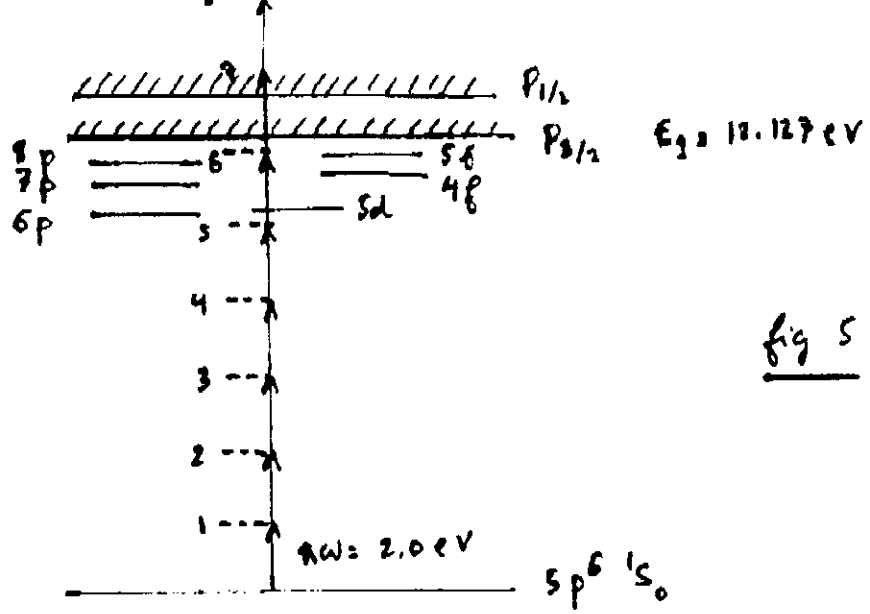

fig 5

V. Intensity and Polarisation dependence in MPI of xenon

We have studied 7-photon ionization of xenon using 120 fs pulses at 615 nm (see lecture 1) for intensities up to 10^{14} Wcm^{-2}. Considering the energy levels in xenon, 6-photon resonances with p and f states are possible as well as 5-photon resonances with s and d states. At low intensity none of these resonances occur but as the intensity is increased they can be Stark-induced, as explained in section II. Since the static detuning of the 5-photon resonances is smaller, they are expected to show at lower intensity. Furthermore, all of these resonances are forbidden by the selection rule $\Delta m = 1$ in circular polarization. In fact, for each circularly polarized photon absorbed by xenon, the angular momentum must increase by one unit, therefore the only possible sequence is $p \to d \to f \to$ etc.. At the 5-photon step all resulting f-photon can be in resonance and the p and f resonances must be suppressed. The laser intensity is monitored for each laser shot. The time-of-flight spectra are stored into 10 bins. This method reduces the

the intensity fluctuations, for a given spectrum by a factor 10 and it provides a scanning of the intensity by small, perfectly controlled, steps. At 10^{13} W.cm^{-2}, the spectrum consists of one peak at about 1.8 eV with a clearly visible structure corresponding to 5-photon resonances and 6-photons resonances corresponding to low static detunings. As the intensity is increased, new peaks appear on the low energy side. The relative amplitudes of the peaks depend on intensity but <u>not</u> their positions. (Fig 6). This is consistant with eqn (8) showing that E does not depend on the laser peak intensity but only on the static detuning and the various Stark coefficients α_R, α_Q, α_P.

Fig 6

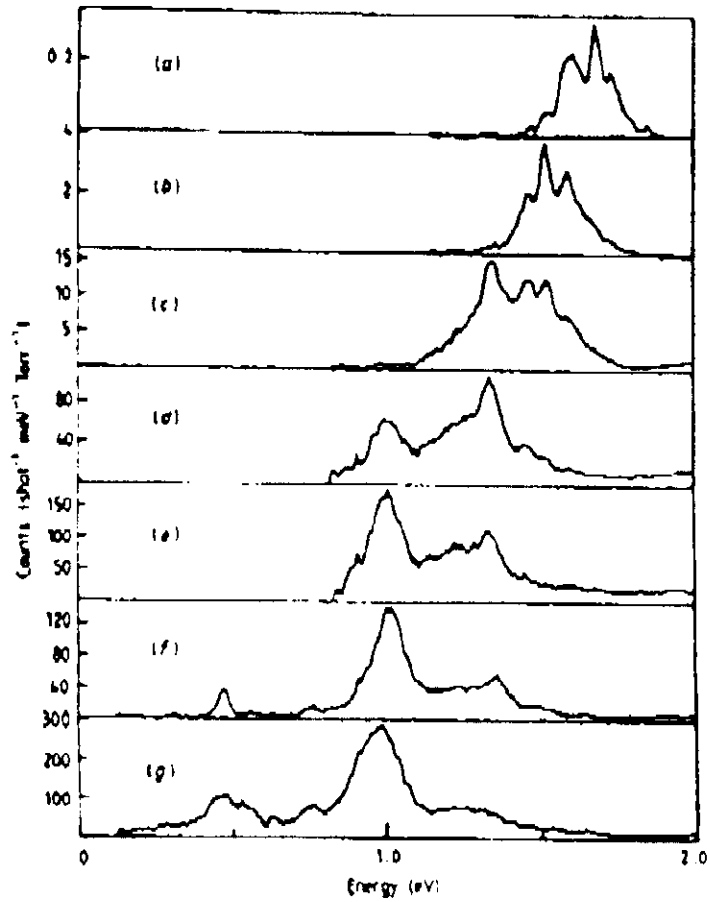

Selected electron energy spectra. The laser intensity increases from 1×10^{13} W cm^{-2} (*a*) to 3×10^{13} W cm^{-2} (*g*).

Figure 7 shows two electron spectra for linear and circular polarizations, at the same laser intensity. In the case of linear polarization the spectrum clearly shows the ATI ($\hbar\omega$) structure but each "peak" is subdivided in a number of substructures two of them being strongly prominent. In circular polarization only the ATI structure remains as discussed above.

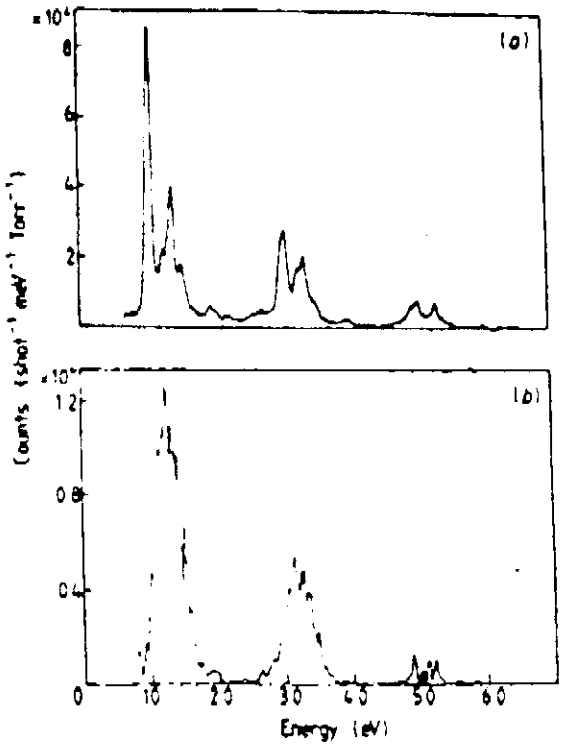

Fig 7

Electron energy spectra for linear (*a*) and circular (*b*) pola
laser intensity.

In order to assign the resonances, it is necessary to know all the relevant Stark shifts. As a first approximation, we can apply the high frequency approximation (3) to estimate the shifts. Neglecting α_g and setting $\alpha_R = \alpha_p$, Eqn (8) reduces to ($N=7$, $p=6$)

$$E = E_R + \hbar\omega - E_I \qquad (9)$$

Hence $E_R = E - \hbar\omega + E_I$. Comparing E_R to known energy values allow, in principle, identification of all resonances.

As shown in the following table, about half of the observed structures can be assigned this way. This was the motivation to try a better approximation by explicitely keeping the $\vec{A}\cdot\vec{p}$ part of the interaction hamiltonian. Under this approximation (still to second order) the shift writes (the term (3) is omitted):

$$\Delta E = - \frac{d}{n^{*3}} \quad \frac{4}{l(l+1)(2l+1)} \langle C_0^{(2)} \rangle \qquad (10)$$

where d is the shift given by (8), l is the orbital momentum and n^* the effective principal quantum number. However, in spite of some changes the main assignments remains with equation (10) since the correction rapidly decreases with n^*.

In order to give more confidence to these assignments it would be useful to follow the perturbed energies $\tilde{E}_n$ as a function of the laser intensity. Hopfully, some kind of extrapolation to zero intensity would support experimentally the results of the calculation. However, as discussed above, the positions of the peaks do not depend on the laser intensity. Therefore, the only free parameter is the static detuning, that is the laser wavelength. This was the basic idea which lead to the tunable femtosecond laser source described in lecture 2 and to the experiment described hereafter.

Table 1. The left column shows the subpeaks' measured energies. When several values are listed on the same line, they correspond to different measurements. The next two columns are lists of the energies and assignments obtained by assuming AC Stark shifts equal to the quiver energy. The rightmost two columns show the energies and assignments obtained from the calculation outlined in the text. We have reported only the results of calculation 2 which differ from those of calculation 1.

Energy			Calc. 1		Assign.	Calc. 2	Assign.
0.311			—		—		
0.353			0.346		$6s^1_{\frac{1}{2}}$		
0.472			0.483		$7s^1_{\frac{1}{2}}$		
0.550			—		—		
0.591			—		—		
0.625			—		—		
0.690			—		—		
0.771					—		
0.820	0.861		0.840		$7p^1_{\frac{1}{2}}$		
0.908	0.911		0.890	0.903	$7p^1_{\frac{3}{2}}$		
0.996	0.989		—		—		
1.019	1.025	1.049	—		—	1.04	$6p^3_{\frac{3}{2}}$
1.08			—		—		
1.171	1.15		1.15	1.16	$4f^1_{\frac{5}{2}}$		
1.205	1.20		—		—		
1.241	1.233		—		—	1.24	$7p^3_{\frac{3}{2}}$
1.283			—		—		
1.327			1.325		$8p^1_{\frac{1}{2}}$		
1.349			1.340		$8p^1_{\frac{3}{2}}$		
1.360			1.364		$8p^1_{\frac{3}{2}}$		
1.410			—		—		
1.471	1.465	1.476	1.469		$5f^1_{\frac{5}{2}}$		
1.505			—		—		
1.540	1.524	1.524	1.560		$9p^1_{\frac{1}{2}}$		
1.590	1.610	1.590	—		—		
1.620			1.634		$9f^1_{\frac{5}{2}}$		
1.684	1.681	1.666	1.690		$10p^1_{\frac{3}{2}}$		
1.940	1.932	1.935	1.940		$9f^1_{\frac{7}{2}}$		
1.809			1.803		$8f^1_{\frac{5}{2}}$		
1.853			1.848		$9f^1_{\frac{5}{2}}$		

VI Linear Giant Stark shifts

We have seen in lecture I that the tunable source we have developped provides wavelength from 570 to 670 nm. The static detuning, for instance for the 7p, can thus be varied by about 1.5 eV. We are interested in $\tilde{E}_R = E_R + \Delta E_R(I)$. For each laser wavelength (or frequency ω) we measure the electron energies corresponding to the 6-photon resonance (as detailed previously). The resonance condition writes:

$$6\hbar\omega = \tilde{E}_R = E_R + \Delta E_R(I) \qquad (11)$$

with, to second order

$$\Delta E_R(I) = \alpha_R I \qquad (12)$$

The photoelectron energy is given by

$$E = 7\hbar\omega - E_I - \Delta E_I(I) \qquad (13)$$

with, neglecting the shift of the ground state

$$\Delta E_I = \alpha_p I \qquad (14)$$

By letting $E_0 = 7\hbar\omega - E_I$ we get

$$I = \frac{E_0 - E}{\alpha_p} \qquad (15)$$

which shows that the measured shift $E_0 - E$ provides a measure of the intensity I. Eliminating I between (15) and (11) provides a relation between measurable quantities:

$$6\hbar\omega = E_R + \frac{\alpha_R}{\alpha_p}(E_0 - E) \qquad (16)$$

Equation (16) summarizes the principle of the method. By plotting $6\hbar\omega$ as a function of $E_0 - E$ one should get straight lines with slopes $\frac{\alpha_R}{\alpha_p}$ extrapolating to E_R for $E_0 - E = 0$, that is for $I = 0$.

Figure 8 shows a typical electron energy spectrum taken at 600 nm. The energy E_0 is indicated (2.34 eV) and the quantity $E_0 - E$ is measured directly on such spectra. The resulting graph $6\hbar\omega = f(E_0 - E)$ is shown in fig. 9.

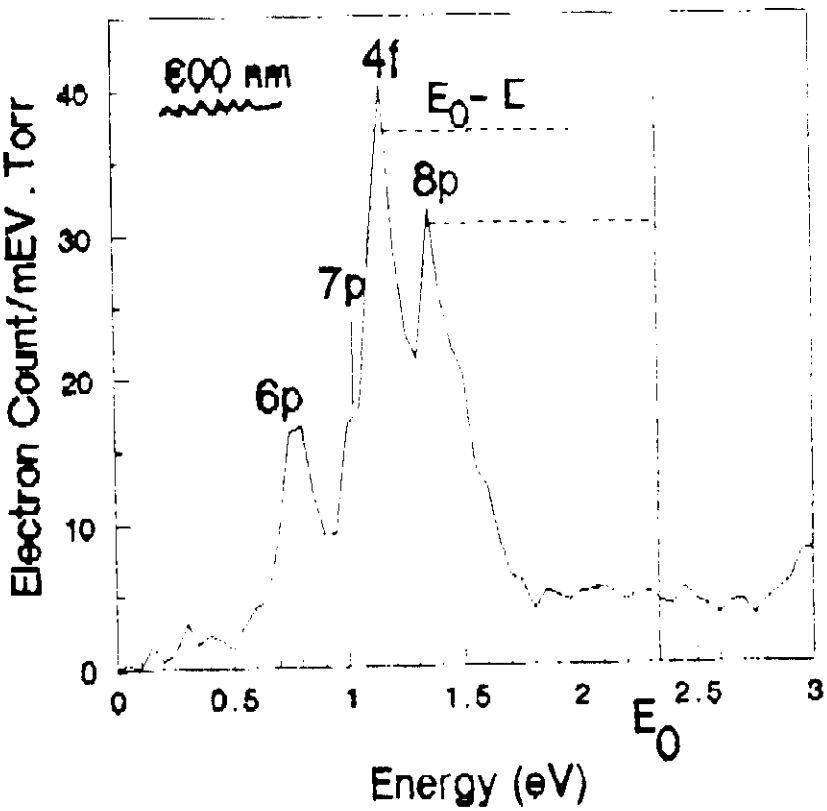

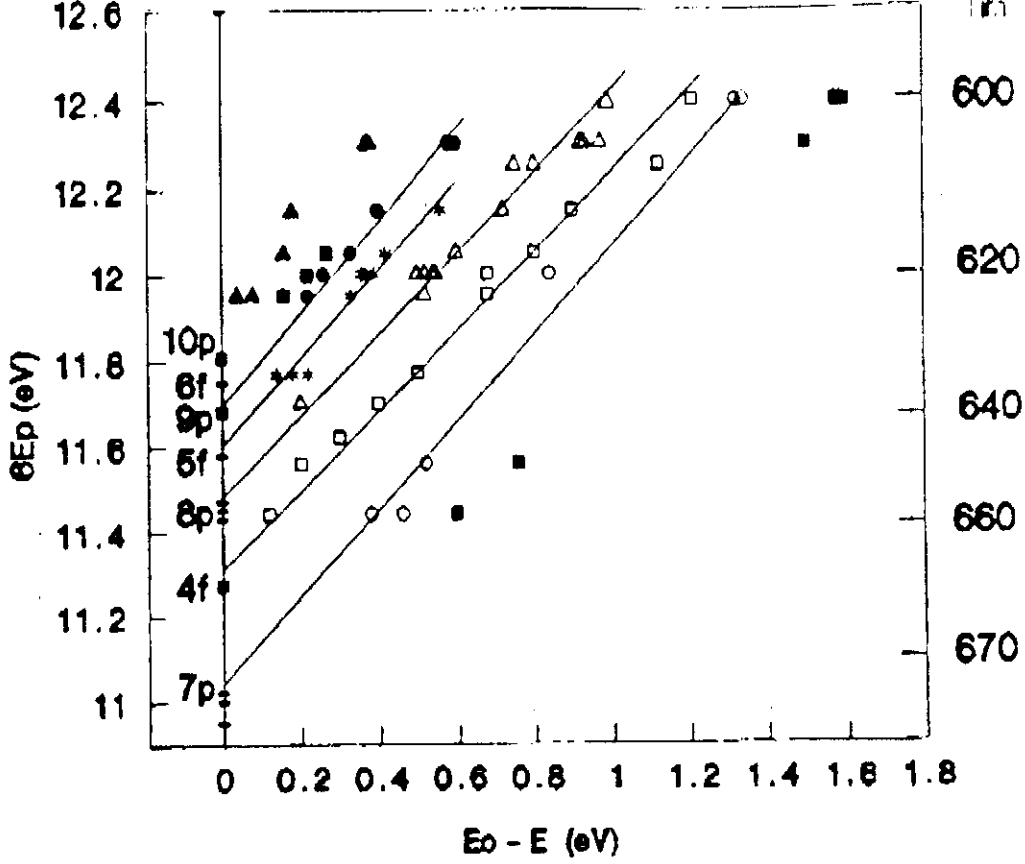

As expected, the experimental points are reasonably aligned on straight lines which do extrapolate towards values which correspond to known energies. This experiment confirms therefore that, around 10^{13} W cm^{-2}, the shifts depend linearly on intensity, as predicted by second-order perturbation theory with coefficients $\alpha_2 \approx \alpha_p$ (the slopes of the straight lines in fig 9 is close to 1). The maximum values of the shifts recorded in this experiment is about 1.5 eV (12000 cm^{-1}) : for instance, fig 8 shows resonances which occur above the unperturbed $P_{3/2}$ continuum limit. The surprising side of this result is that the shifts are linear with intensity. This is especially unexpected for p states which are strongly coupled to autoionizing state s' and d' between

the $P_{3/2}$ and the $P_{1/2}$ limits. Figure 10 shows the result of a second-order Stark shift calculation for the 7p[1/2], J=0 state. The wavefunctions are derived from a MQDT analysis which was tested on a number of known results. The shift is shown as the dashed line and displays, as expected, a number of dispersion-like features due to resonant coupling of the 7p to the 9s', 10s', 11s' and 8d', 9d' state. However, by convoluting this function with the laser linewidth function, one gets the solid line which, within the experimental error bar, coincides with the ponderomotive shift shown as the dotted line.

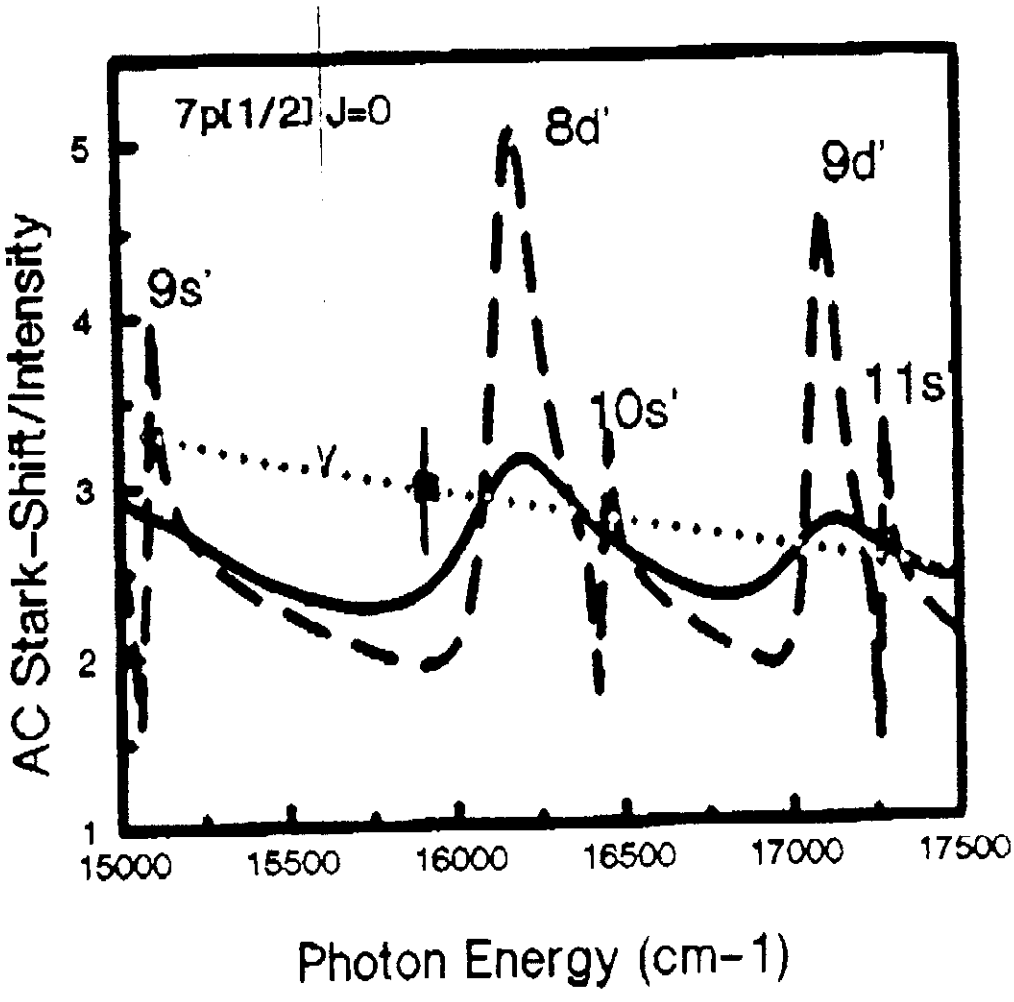

In spite of the fact that second-order calculations seem to account reasonably well for the observed shifts, the validity of such calculations at 10^{13} W cm^{-2} is highly questionable. However, such calculations are surely valid at low intensity, that is around $E_0 - E = 0$. The resulting α_p, close to α_p, even for states like the 7p support our extrapolation to zero. What is the most likely explanation of what is observed is the following, according to recent non-perturbative calculations (Floquet-type): at low intensity such calculations, naturally agree with second-order perturbation theory. At higher intensity there is a range where the shifts are non linear and the state strongly mixed. At even higher intensities however, it means that what can be defined as a <u>diabatic</u> continuation of state shifts <u>linearly again</u> with intensity, with coefficients close to α_p.

Of course such qualitative statement, derived from calculations in Hydrogen must be confirmed in specific cases in reality and the above results must be considered as preliminary.

References

Stark-induced resonances in MPI

Y. Gontier, N. K. Rahman and M. Trahin Phys. Rev. Lett 34, 779 (1975)

P. Kruit, J. Kimman, H. G. Muller and M. J. Van der Wiel J. Phys. B: At. Mol. Phys 16, 973 (1983)

M. Poirier, J. Reif, D. Normand and J. Morellec J. Phys. B: At. Mol. Phys 17, 4135 (1984)

R. Freeman, P. H. Bucksbaum, H. Milchberg, S. Darack, D. Schumacher and M. Geusic Phys. Rev Lett 21, 1092 (1987)

P. Agostini, A. Antonetti, P. Breger, M. Crance, A. Migus, H. G. Muller and G. Petite J. Phys. B: At. Mol. Phys 22, 1971 (1989)

P. Agostini, P. Breger, A. L'Huillier, H. G. Muller and G. Petite A. Antonetti and A. Migus
Phys. Rev. Lett. 63, 2208 (1989).

A. Szöke, O. L. Landen and M. D. Perry Phys. Rev. A 40, 2766 (1989)

M. D. Perry, A. Stoke and K. C. Kulander Phys. Rev. Lett 63, 1058 (1989).

Stimulated Radiative Corrections

E. Arnous, J. Bastian and A. Maquet Phys. Rev A 27, 973 (1983) and ref. therein.